This is the accepted version of the following article: [Lequoy, P. , Liberelle, B. , De Crescenzo, G. and Lerouge, S. (2014), Additive Benefits of Chondroitin Sulfate and Oriented Tethered Epidermal Growth Factor for Vascular Smooth Muscle Cell Survival. Macromol. Biosci., 14: 720-730], which has been published in final form at https://doi.org/10.1002/mabi.201300443. This article may be used for non-commercial purposes in accordance with the Wiley Self-Archiving Policy [olabout.wiley.com/WileyCDA/Section/id820227.html].

Public access - Manuscript accepted

Published in final edited form as: Macromol Biosci. 14 (5), 720-730, 2014 (doi.org/10.1002/mabi.201300443)

Additive benefits of chondroitin sulfate and oriented tethered Epidermal Growth Factor for vascular smooth muscle cell survival

Pauline Lequoy[a], Benoît Liberelle[b], Gregory De Crescenzo[b,*] and Sophie Lerouge[a,*]

[a] Research Centre, Centre Hospitalier de l'Université de Montréal (CRCHUM). 1560 rue Sherbrooke Est, Montréal (QC), Canada H2L 4M1.

and

Department of Mechanical Engineering, École de technologie supérieure (ÉTS). 1100 boul. Notre-Dame Ouest, Montréal (QC), Canada H3C 1K3.

[b] Department of Chemical Engineering, École Polytechnique de Montréal. P.O. Box 6079, succ. Centre-Ville, Montréal (QC), Canada H3C 3A7.

(*) Corresponding authors - both authors contributed equally to this work.

E-mail: sophie.lerouge@etsmtl.ca; Tel: +1 514 890 8000 (# 28821); Fax: +1 514 412 7785.

E-mail: gregory.decrescenzo@polymtl.ca; Tel: +1 514 340 4711 (#7428); Fax: +1 514 340 2990.

Abstract

An anti-apoptotic coating for vascular applications combining chondroitin sulfate (CS) and coiled-coil-based tethering of epidermal growth factor (EGF), a key growth factor involved in wound healing, was designed. EGF quantification by ELISA showed that higher protein surface densities were reached using the oriented tethering strategy compared to the commonly used random covalent grafting, while using much lower concentrations of EGF during incubation. Vascular smooth muscle cell (VSMC) survival and resistance to apoptosis in serum-free conditions were significantly improved on CS surfaces exposing oriented EGF compared to random EGF. The comparison of CS and low-fouling carboxymethylated dextran as a sublayer for growth factors highlighted the tremendous benefit of CS thanks to its selective protein resistance and good cell adhesion properties. While this bioactive coating was specifically designed to promote healing around stent-grafts for endovascular aneurysms repair (EVAR), the approach undertaken can be tuned for other applications, e.g., by capturing other GFs through coiled-coil interactions.

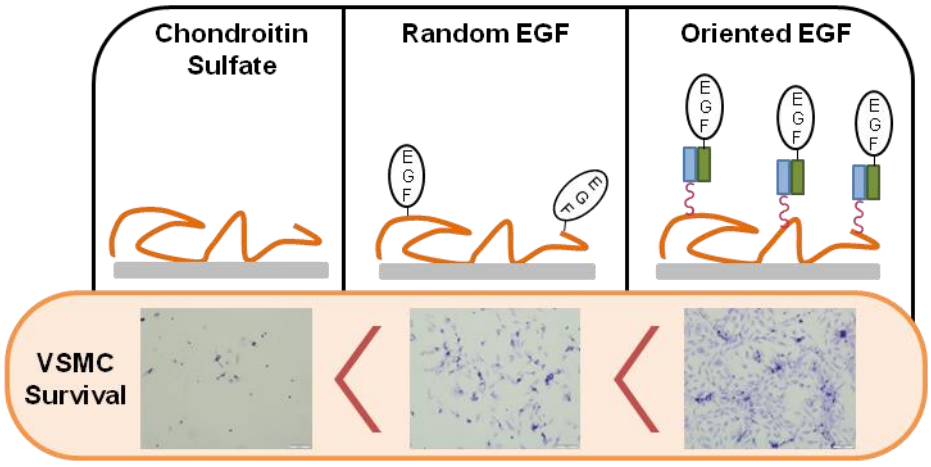

1. Introduction

Bioactive coatings are increasingly used to overcome the limitations of conventional biomaterials possessing good mechanical properties but insufficient biocompatibility [1, 2]. This is particularly true for PET and PTFE-based cardiovascular implants, such as stent-grafts (SG), employed for the endovascular treatment of abdominal aortic aneurysms (AAA) [3]. While PET and PTFE surface properties appear adequate to avoid thrombosis on the luminal side of the SG, the lack of healing around the implant is a major factor leading to clinical complications [4-6]. This deficient healing is due to several concomitant factors: 1) the bio-inertness of PET and PTFE, 2) the pre-existent context of the aneurismal vessel, such as vascular smooth muscle cell (VSMC) depletion and pro-apoptotic phenotype [7, 8] as well as extracellular matrix (ECM) proteolytic degradation [9, 10], and 3) the deprivation of nutrients and oxygen once the SG excludes the aneurysm from blood flow.

Recently, we have developed a bioactive coating specifically designed to trigger adequate vascular cell response while counteracting the mechanisms occurring after SG insertion [11-13]. In order to favor vascular cell growth and resistance to apoptosis around the SG, we proposed to combine two biomolecules, namely chondroitin sulfate (CS) and epidermal growth factor (EGF). CS, a glycosaminoglycan naturally encountered in blood vessels, has demonstrated anti-apoptotic properties through ERK1/2 phosphorylation and enhanced Bcl-xl expression in rat and human VSMC [14] as well as in fibroblasts [15]. This widely available glycosaminoglycan has also been shown to favor wound healing by improving cell migration, increasing fibronectin synthesis and promoting fibroblast proliferation [16, 17]. EGF is one of the key growth factors involved in wound healing [18, 19] and is known to promote VSMC proliferation [20-22]. Of interest, activation of EGF cell receptors also initiates specific anti-apoptotic signals, by

activation of PI3K/AKT, RAS/ERK and JAK/STAT pathways, leading to an increased release of anti-apoptotic proteins and a decreased release of pro-apoptotic proteins [23-25]. When an EGF layer was covalently grafted on CS via carbodiimide chemistry, the resulting coating was found to possess anti-apoptotic and pro-proliferative properties for rat aortic VSMC [12, 13].

However, random covalent EGF coupling can negatively impact protein bioactivity due to inappropriate orientation and/or epitope inactivation, thus preventing optimal interactions with cells [26, 27]. We hypothesized that the bioactivity of a coating including CS and EGF could be further enhanced by the use of oriented EGF immobilization, where all immobilized EGF molecules are attached via a tag added to a specific EGF region in order to allow immobilization without epitope inactivation. In that purpose, our group recently developed an innovative oriented immobilization strategy for growth factors based on two high affinity peptides, namely Ecoil and Kcoil, that heterodimerize with high specificity and affinity [28]. Ecoil-tagged epidermal growth factor (Ecoil-EGF) was produced in human embryonic kidney (HEK) 293 cells and its bioactivity was confirmed on human epidermoid carcinoma (A-431) and human corneal epithelial (HCE-2) cell lines [27, 29]. Here, we show that EGF can be immobilized on CS via a coiled-coil strategy (**Fig. 1**), with large benefits compared to random immobilization in terms of protein surface density and bioactivity, as assessed by direct ELISA, VSMC survival and resistance to apoptosis in a serum-deprived environment. Moreover, to demonstrate the benefit of CS in this bioactive coating, we studied in parallel the bioactivity of EGF immobilized on CS coatings and on another commonly-used protein resistant polysaccharide, carboxymethylated dextran (CMD) [30].

This work was achieved using aminated microplates for protein quantification and cell culture tests as a model for vascular implant materials, knowing that primary amine groups can readily

be created on PET and PTFE via plasma polymerization, plasma functionalization or using aminolysis of PET [13, 31-34], and that the strategy could later be easily transferred to realistic biomaterial surfaces.

2. Materials and methods

2.1. Materials and reagents

Native silicon wafers (Prime Si P/Boron) were obtained from University Wafer (South Boston, MA). Anhydrous 3-aminopropyltriethoxysilane (APTES, 99% purity), acetic acid (99.7% purity), cysteine (99+% purity), glutaric anhydride (95% purity), sodium chloride (99.99% purity), N-(3-dimethylaminopropyl)-N'-ethylcarbodiimide hydrochloride (EDC), N-hydroxysuccinimide (NHS), 2-morpholinoethane sulfonic acid (MES), Dulbecco's Phosphate Buffered Saline (modified PBS, without calcium chloride and magnesium chloride), Tween 20 and cysteine (99+% purity) were purchased from Sigma-Aldrich (Oakville, ON). EMCH (3,3´-N-[***ε***-maleimidocaproic acid] hydrazide, trifluoroacetic acid salt) was purchased from Pierce Biotechnology (Rockford, IL). Commercially available DuoSet ELISA kit containing mouse anti-human EGF antibody (capture antibody), biotinylated goat anti-human EGF antibody (detection antibody), streptavidin-horseradish peroxidase (streptavidin-HRP), bovine serum albumin (BSA), substrate solution (hydrogen peroxide/tetramethylbenzidine) and untagged recombinant human EGF were purchased from R&D Systems (Minneapolis, MN).

2.2. Kcoil and Ecoil-tagged EGF Production

Cysteine-tagged Kcoil peptides [28] were synthesized by the peptide facility at University of Colorado (Denver, CO). The chimeric Ecoil-EGF, formed by an EGF molecule with an Ecoil

peptide attached to its N- terminus, was produced in HEK 293-6E cells and purified by immobilized metal-ion affinity chromatography (IMAC) as previously described [28]. Protein concentration was determined by ELISA. Purified Ecoil-EGF was then stored at -80°C until use.

2.3. CS, CMD and EGF Immobilization

2.3.1. Surface and Polymer Preparation

Aminated silicon surfaces and microplates were used for chemical grafting characterization and cell culture assays, respectively. Amino groups were created on silicon wafer surfaces (1×1 cm) via an APTES-based silanization procedure [12]. Aminated microplates (96-well Clear Polystyrene Amine Surface Stripwell Microplate, Corning Inc.) were purchased from Fisher Scientific (Ottawa, ON). For cell culture experiments, microplates were disinfected by exposure to 70% EtOH for 5 min before EGF or Ecoil-EGF immobilization. Carboxymethylated dextran (CMD) chains were generated from commercially available dextran (Pharmacosmos, Holbaek, Denmark) by adapting previously reported protocols [27]. Under our experimental conditions, the carboxymethylation degree of the dextran chains (500 kDa) was 55%. Chondroitin-4-sulfate (CS) was purchased from Sigma–Aldrich (Oakville, ON). Lyophilized CMD and CS powders were stored at 4°C until use.

2.3.2. Polymer Grafting on Aminated Silicon Surfaces and Aminated Microplates

CMD and CS were covalently attached onto amino-coated surfaces using water-soluble carbodiimide chemistry, according to previously reported protocols [13, 27]. CMD solution was prepared in Milli-Q water (2 mg/mL). Once dissolved, CMD was activated by preparation of a solution containing (for 1 mL): 100 µL of 0.4 M EDC in Milli-Q water and 100 µL of 0.1 M NHS to 800 µl of CMD solution [27]. CS was dissolved in Milli-Q water at 0.1 g/mL, and the

resulting solution was filtered (0.2 µm PTFE filter) to remove aggregates. CS was then activated by preparing a solution containing (for 1 mL): 400 µL of EtOH 100%, 347 µL of Milli-Q water, 50 µL of 1 M MES, 57 µL of 0.4 M EDC, 46 µL of 0.1 M NHS, and 100 µL of CS solution [13]. The NHS-activated polymer solutions were reacted with the aminated surfaces (150 µL/cm^2) and microplates (100 µL/well) for 1h. The surfaces and the wells were finally rinsed once using PBS (10 mM, pH 7.4) and two times using Milli-Q water for 2 min in an ultrasonic bath.

2.3.3. EGF Covalent Immobilization on CMD- and CS-coated surfaces

The CMD-coated surfaces were activated with 100 µL of a solution containing (for 1 mL): 500 µl of 0.4 M EDC and 500 µl of 0.1 M NHS for 15 min [27] and the CS-coated surfaces were activated with 100 µL of the following solution (for 1 mL): 400 µL of 100% EtOH, 497 µL of Milli-Q water, 57 µL of 400 nM EDC, 46 µL of 100 nM NHS [13]. The surfaces were rinsed with Milli-Q water. NHS-activated polymer surfaces were then exposed to 100 µL of untagged EGF (in 10 mM PBS pH 7.4 containing 0.05% Tween 20, PBS-T) for 1 h. Finally, the surfaces were rinsed with PBS and Milli-Q water.

2.3.4. Ecoil-Tagged EGF Capture on Kcoil Layers

A Kcoil layer was generated on CMD or CS-covered surfaces using EMCH linker, which possesses an amine group at one end and a maleimide group at the other end. CMD and CS carboxylic groups were activated using NHS/EDC-based chemistry as described in section **2.3.3.** The NHS-activated polymer layers were then reacted with the amine group of EMCH by depositing 100 µL of 1 mM (0.41 mg/mL) EMCH in PBS:DMSO (90:10 v/v) on each surface for 30 min. The surfaces were rinsed using PBS and Milli-Q water. Deactivation of remaining polymer COONHS groups was obtained with 100 µL ethanolamine solution (1 M, pH 7.0) for 15 min, followed by rinsing with PBS and Milli-Q water. Thiol-reactive surfaces were then reacted

with 100 µL of 10 µM cysteine-tagged Kcoil in Milli-Q water for 1 h. The surfaces were rinsed using PBS and Milli-Q water. Unreacted sites of EMCH were blocked using 100 µL of 50 mM cysteine solution (1 M NaCl in 0.1 M sodium acetate, pH 4.0) followed by rinsing with PBS and Milli-Q water. Surfaces harboring covalently bound Kcoil were incubated with 100 µL of Ecoil-EGF solution (in 10 mM PBS pH 7.4 containing 1% BSA, PBS-BSA) for 1 h. After the Ecoil-EGF capture, the wells and the surfaces were rinsed using PBS. When needed, Ecoil-EGF was detached by soaking the Ecoil-EGF-covered surfaces in a 5 M guanidium hydrochloride solution (Gnd-HCl), followed by rinsing with PBS and Milli-Q water.

2.4. Physical and chemical characterization

2.4.1. Ellipsometry

Dry thickness of grafted layers on APTES-coated silicon wafers was measured using an automatic M2000 ellipsometer (J.A. Woollam, Lincoln, NE) equipped with data acquisition software (Complete EASE). The measurements were performed with a 75° angle of incidence and data were acquired within a wavelength range of 245-1650 nm. A refractive index of n = 1.465 was used for the measurements of APTES, CS, Kcoil and Ecoil-EGF layers [12]. The dry thickness of each layer was obtained using the WVase 32 analysis software package and defined as the difference between the APTES-coated silicon wafers and the CS-, Kcoil- and Ecoil-EGF-coated wafers. Three measurements were taken on each surface and the experiment was repeated at least twice.

2.4.2. Water contact angle

Wettability of the coatings was measured through static contact angle with a FTA200 goniometer (First Ten Ångstroms, Portsmouth, VA) equipped with a data analysis software

package (FTA32 Video). Three measurements were taken on each surface using Milli-Q water as probe liquid and the experiment was repeated at least twice.

2.4.3. Surface EGF quantification by ELISA

Quantification of EGF surface densities in the wells was performed by direct ELISA. The wells were first incubated with 100 µL of a biotinylated anti-human EGF antibody (50 ng/mL in PBS-BSA) for 30 min. The wells were washed 3 times with PBS-T and 100 µL of a streptavidin-HRP solution (diluted 200 times in PBS-BSA) was added to the wells for 20 min. Finally, the wells were rinsed 3 times with PBS-T and reacted with 100 µL of the substrate solution (mixture of hydrogen peroxide and tetramethylbenzidine). The optical density (OD) at 630 nm was measured using an ELISA plate reader (Victor ^{3}V Multilabel Counter, PerkinElmer, Woodbridge, ON). The slopes corresponding to the OD variation in the wells over time, were compared to those obtained with known concentrations of EGF.

2.5. Cellular assays

2.5.1. Cell culture materials

Vascular smooth muscle cells (VSMC) from rat embryonic thoracic aorta (a7r5 cell line, ATCC, Manassas, VA) were cultured under 15 passages in Dulbecco's Modified Eagle's Medium/Nutrient Mixture F-12 Ham's Media (DMEM/F12; Invitrogen, Burlington, ON) supplemented with 10% fetal bovine serum (FBS; Medicorp, Montreal, QC). DMEM/F12 supplemented with 1% penicillin-streptomycin (Pen-Strep; Invitrogen, Burlington, ON) was used as serum-free medium in survival and apoptosis experiments. Tissue culture-treated polystyrene (PS) 96-well plates (Corning Inc., Corning, NY) were used as a positive control.

2.5.2. Cell survival in serum-free medium

VSMCs were seeded at 20 000 cells/well in microplate wells and incubated on each surface at 37°C and 5% CO_2 in 200 µL of complete growth medium (DMEM/F12 + 10% FBS and 1% Pen-Strep). After a 24h adhesion period, the surfaces were rinsed with PBS to detach non-adherent cells; and serum-free medium was added (200 µL/well) and changed every two days. For conditions designated as 'soluble EGF', 10 ng/mL of EGF was supplemented in the culture medium [12]. Cell metabolic activity was probed using the alamarBlue assay (Invitrogen, Burlington, ON). Once rinsed with 200 µL of PBS, the wells were exposed to alamarBlue added to the culture medium (10% v/v) for 4h. AlamarBlue fluorescence signal was read using a spectrophotometer (560 and 590 nm, for excitation and emission wavelengths, respectively). Cell density and homogeneity on the well surfaces were evaluated via crystal violet staining (Fisher Scientific, Ottawa, ON), i.e. cells were incubated in a crystal violet solution (0.075% w/v in 3% v/v acetic acid solution) for 15 min, rinsed 3 times with Milli-Q water and air-dried prior to capture (Leica Microsystems, Richmond Hill, ON). At least three samples per conditions were used and each experiment was performed in duplicate.

2.5.3. Cell apoptosis

VSMCs were seeded at 20 000 cells/well in microplate wells and incubated on each surface at 37°C and 5% CO_2 in 200 µL of complete growth medium (DMEM/F12 + 10% FBS and 1% Pen-Strep). After an 8h adhesion period, half of the plate was exposed to complete growth medium for 14h (positive control), while the other half-plate was exposed to serum-free medium for 14h to induce apoptosis. To be noted, several time points were tested for serum-free medium exposure but 14h was selected as the shortest time point at which statistical differences in apoptotic cell numbers were observed with a comparable total number of cells on the surfaces. Resistance to apoptosis in serum-free conditions was assessed by a Hoescht 33342

(HT)/propidium iodide (PI) staining test [12]. Briefly 1 µg/mL of HT (Sigma-Aldrich, Oakville, ON) and 5 µg/mL PI (Invitrogen, Burlington, ON) were directly incorporated into the medium of each well. Images were captured after a 5-min incubation time using fluorescence microscopy (excitation filter of 360–425 nm). At least three samples per condition were used and each experiment was performed in duplicate.

2.6. Statistical analysis

Results are expressed as mean ± standard deviation ($n \geq 3$). Statistical analysis was carried out using independent two-sample t-test with equal variances. A *p*-value lower than 0.05 was considered significant for all tests.

3. Results

3.1 Characterization of oriented EGF immobilization on CS via coiled-coil interaction

Grafting steps for the oriented immobilization of EGF on CS-coated silicon wafers (**Fig. 1**) were characterized using ellipsometric dry thickness (**Fig. 2**) and water contact angle measurements, as previously reported for the random EGF grafting on CS and CMD polymers as well as for the oriented EGF immobilization on CMD [12, 27]. Amino groups were created on silicon wafers via an APTES-based silanization procedure. The APTES layer was found to be thick, homogeneous and relatively hydrophobic, showing a water contact angle of 70.7 ± 2.8° and an ellipsometric thickness of 4.75 ± 0.16 nm (condition **a** on **Fig. 2**, to be compared to native silicon wafers, i.e. 0 nm and 0°). Grafting of the hydrophilic CS layer via carbodiimide chemistry induced a decrease in contact angle to 51.1 ± 3.4° and an increase in dry thickness of 0.37 nm (condition **b**) compared to the APTES layer (condition **a**). Following CS immobilization, contact

angle remained stable throughout the rest of the grafting process (data not shown). Immobilization of EMCH linker on CS was followed by Kcoil grafting by reaction of EMCH maleimide groups with the thiol terminal group of Kcoil peptide (+0.10 nm, condition **c**). The reversibility of the E/K coiled-coil interaction was demonstrated in two steps: first, the capture of Ecoil-EGF by incubation of a 600 nM-solution (in 10 mM PBS, pH 7.4) on Kcoil-functionalized surfaces, then the detachment of Ecoil-EGF thanks to a chaotropic agent (5 M Gnd-HCl). This led to net dry thickness variations of +0.38 nm and –0.40 nm, respectively (conditions **d** and **e**). Ecoil-EGF (600 nM) was also incubated on EMCH layers that had previously been blocked by cysteine molecules (condition **f**). Absence of thickness gain in this case (compare conditions **f** and **g**) confirmed that Ecoil-EGF is only recruited via the specific coiled-coil interactions.

3.2 ELISA quantification of immobilized EGF

The ability to control the EGF surface density in both oriented and random strategies was studied on CS and CMD via direct ELISA by varying EGF incubation concentration from 315 pM to 900 nM (**Fig. 3**). Fine-tuning of EGF incubation concentrations was performed to ensure similar EGF densities on both polysaccharide-coated surfaces during cell experiments and thus ease comparison. It should be noted that ELISA quantification relies on both the presence and the orientation of EGF on the surface, as the ELISA detection antibody is sensitive to a specific epitope of the EGF protein that might not be accessible for all immobilized EGF molecules. Therefore, the surface densities in **Fig. 3** characterize the amount of bioavailable EGF, rather than the total quantity of immobilized EGF.

For the oriented grafting strategy on CS, the maximal surface density (45 fmol/cm^2) was obtained with an Ecoil-EGF incubation concentration of 22 nM. The same density was reached

on Kcoil-functionalized CMD with an Ecoil-EGF concentration of 625 pM. In contrast, the EGF surface density obtained by random coupling on CS was lower despite the use of considerably higher incubation concentrations, i.e 1.5 fmol/cm^2 for incubation concentration of 900 nM EGF. To achieve the same surface density on CMD, a concentration of 300 nM EGF was required. Thus, compared to EGF random grafting, the coiled-coil system not only enabled to reach higher EGF surface densities, but it also increased grafting yield, insofar as ca. 1000-fold less EGF was needed to achieve the same surface density. That is, an EGF density of 1.5 fmol/cm^2 was immobilized on CS with 1.5 nM of Ecoil-EGF or with 900 nM of untagged EGF (**Fig. 3**).

EGF non-specific adsorption was evaluated by incubation of untagged EGF (100 nM in PBS for 1h) on wells that had been coated with 1) CS and 2) CMD, as well as on 3) pristine aminated wells as control. As can be seen in **Table 1**, EGF adsorption was found to be similar on CS- and CMD-covered wells (0.077 and 0.070 fmol/cm^2, respectively, $p = 0.62$) and drastically higher on pristine aminated wells (0.934 fmol/cm^2, $p < 0.001$ compared to CS and CMD). This result demonstrates that CS and CMD layers are equally efficient to reduce EGF adsorption and that the polymer layers are sufficiently dense and homogeneous to mask the underlying aminated wells. The featured low-fouling properties of CS confirm previous results by Keuren et al. [35] showing low adhesion of plasma proteins such as fibrinogen, albumin and antithrombin on CS-covered surfaces. In the context of a bioactive coating, CS low-fouling properties could prevent protein aggregation and therefore improve the exposure of grafted growth factors to cells from the vessel wall.

3.3 Bioactivity of the coatings

Cell survival and apoptosis were assessed to estimate the bioactivity of the various EGF layers immobilized on CS and CMD. For all tests, EGF proteins were grafted on CS at the

maximal surface densities, i.e. 45 fmol/cm^2 and 1.5 fmol/cm^2 for oriented tethering and random grafting, respectively. As a consequence, each immobilization technique was tested at its full potential, with the highest surface density achievable (see **Figure 3**). The concentrations of the grafting solutions were then adjusted for CMD coatings to reach the same EGF surface densities in order to evaluate the influence of the polymer underneath EGF (CS vs CMD).

3.3.1 Cell adhesion and survival

VSMC were cultured on the different coatings for 24h in complete growth medium (adhesion at day 0) and then exposed to serum-free medium for 3, 5 and 7 days. Polystyrene (PS) and pristine aminated wells were used as controls. **Fig. 4** presents the cell adhesion (in %) expressed as the day 0 alamarBlue signal obtained on the coated surfaces normalized to the one on PS surfaces. **Fig. 5** presents the cell survival (in %) after 3, 5 and 7 days in serum-free medium on each surface after normalization to their respective initial alamarBlue signal at day 0. The consistency of the alamarBlue results with the number of cells on the surface was confirmed by crystal violet staining (**Fig. 6**).

After the 24h-incubation, high cell adhesion was observed on CS-coated and pristine aminated wells (ca. 145% of adhesion on PS), and EGF grafting on CS did not affect cell adhesion compared to bare CS (**Fig. 4**). Despite similar EGF-resistance properties (**Table 1**), CMD and CS displayed very different cell-adhesive properties, since cell adhesion was found to be low on CMD, with an alamarBlue signal on CMD layers being 25% of that obtained for CS-coated surfaces at day 0 ($p < 0.005$).

Upon exposure to serum-free medium, VSMC survival on both PS and pristine aminated surfaces showed a progressive decrease over time from 100% (day 0) to ca. 45% (day 7), suggesting that the surface-exposed amine groups do not influence the cell survival (**Fig. 5**). The

same trend was observed for CS-coated wells with a cell survival of 45% at day 7, confirming that CS *per se* does not improve the cell survival over 7 days compared to tissue culture PS [13]. When soluble EGF was supplied in the serum-free medium, the survival was enhanced on PS and CS-coated wells to ca. 80% (day 7), indicating that EGF triggered cell survival mechanisms, as expected [13, 23]. Despite similar initial cell adhesion (**Fig. 4**), a clear behavior discrepancy was observed in serum-free conditions between bare CS and CS covered with random or oriented EGF (**Fig. 5**). Cell survival slowly decreased over time on bare CS and randomly grafted EGF layers, i.e. 87, 70, 45% and 96, 82, 66%, respectively (for day 3, 5, 7) ($p < 0.05$ at day 7). The slower decrease in cell density observed for random EGF coatings compared to bare CS confirmed that immobilized EGF improved the cell survival on CS, as previously featured [13]. In stark contrast, after 7 days in serum free conditions, cell density was maintained for the coiled-attached EGF layers to ca. 106% compared to day 0. This confirms that EGF oriented immobilization offered an important additional asset by preventing cell depletion in serum-free conditions, as also highlighted in **Fig. 6.** Contrarily to CS-coated surfaces, EGF grafting on CMD layers did not improve VSMC survival. Indeed, negligeable signals were detected as of day 3 (**Fig. 5**) on all CMD-based coatings, indicating that the presence of EGF was not sufficient to counterbalance the low-fouling, cell-repellent properties of the CMD underlayer (also featured in **Fig. 6**).

3.3.2. Cell apoptosis.

In order to explain the superiority of the CS and oriented EGF combination observed in VSMC survival, cell resistance to apoptosis was assessed on the different surfaces after 14h in serum-free medium using Hoescht 33342/propidium iodide staining (**Fig. 7**). Viable, apoptotic and necrotic cells were identified according to cell morphology and color, as previously

described [12, 13]. Regardless of the surface coating, we observed that serum-free medium favored apoptosis when compared to complete growth medium, while necrosis remained very low (≤ 1% in serum-free medium and complete medium). The proportion of VSMC presenting an apoptotic phenotype was significantly lessened on CS surfaces compared to pristine aminated and PS wells (9, 14 and 16%, respectively, with $p < 0.005$), confirming that a coating of CS initiated anti-apoptotic mechanisms for VSMC [12, 13]. Random EGF tended to further decrease apoptosis but no statistical difference was established between bare CS and random EGF on CS ($p = 0.2$), as previously reported [13]. However, apoptosis was significantly reduced when the EGF was displayed in an oriented fashion on the CS compared to bare CS surface (6 and 9%, respectively, with $p = 0.01$). This better resistance to apoptosis induced by CS when allied to the known pro-proliferative role of EGF [20-22] could have compensated the number of cells lost by apoptosis during the 7-day treatment in serum free medium, and appears as the likely origin of the excellent VSMC survival seen in **Fig. 5**.

4. Discussion

VSMC survival in pro-apoptotic conditions (e.g. serum starvation, hypoxia) is a key issue in the case of aortic aneurysms after implantation of a stent-graft. Indeed, the VSMC apoptosis and depletion that characterize aneurismal vessel walls combined with poor access to nutrients and oxygen following SG implantation, are believed to play a major role in the lack of healing observed around SGs [7, 8]. While the thrombus formed in the aneurismal cavity after deployment of SG should ideally evolve in an organized fibrous tissue encapsulating the implant and contract to induce aneurysm shrinkage, explanted SG are most often found surrounded by an unorganized blood clot with a strong deficit in fibroblasts, VSMC and collagenous ECM, even

after years of implantation. This lack of integration of the SG in the vessel wall [4, 6] causes frequent complications such as migration or endoleaks [36].

Currently, the solutions proposed by manufacturers to prevent SG migration and endoleaks are design features that provide mechanical - but not biological - attachment, such as the use of metal hooks that anchor the SG in place and the use of oversized terminal rings at the necks to seal the ends [37]. In parallel, a few research groups have been working on improving the healing around SGs, most of them by using fibroblast growth factor (FGF) to increase fibroblast and VSMC growth as well as collagen production [38-40]. Those coatings combining FGF, heparin and collagen [38] or FGF and elastin [39] have induced an interesting neointima formation in vivo in healthy vessels of pigs and dogs, respectively. However their ability to address cell apoptosis in a complex diseased environment with limited access to nutrients and growth factors, has not been considered.

To induce tissue ingrowth on the abluminal surface of the SG, VSMC and fibroblasts must either cross the thrombus formed between the implant and vessel wall or migrate along the implant surface from the proximal and distal necks of the aneurysm where the SG is in contact with the host vessel wall. The cells must adhere on the implant external surface, proliferate and survive to the unfavorable, pro-apoptotic environment. Yet, PTFE and PET used in SG either trigger oxidative stress leading to cell death by anoikis [41] or fail to activate appropriate survival signals. Our general aim is to design a bioactive coating that would favor the integration of the implant in the tissue and reduce clinical complications by promoting the adhesion, proliferation, migration and survival of VSMC and fibroblasts.

CS and EGF were chosen since these biomolecules are both involved in vascular repair after injury, promoting anti-apoptotic phenotypes of the vascular cells involved in fibroproliferative

reactions (vascular smooth muscle cells, fibroblasts, mesenchymal stem cells) [14, 15, 25]. EGF is also well known to promote cell proliferation and migration [20, 42-44]. Excessive fibroproliferative responses are detrimental in several vascular pathologies such as atherosclerosis or restenosis after stent implantation [45, 46]. Nevertheless, proliferative response occurring on the external surface of a SG could be beneficial to improve its integration and fixation to the aneurismal wall. The present data confirmed that a coating combining CS and EGF favors cell adhesion and survival in serum-free medium mimicking nutrients deprivation after SG implantation but also showed that the coating bioactivity was largely improved by oriented tethering of EGF on CS (**Fig. 4 to 7**). Thanks to the high efficiency of capture of our coiled-coil tethering system, a dense coverage of optimally-oriented growth factor can be produced, while drastically reducing the amount of growth factor needed, when compared to random covalent grafting (**Fig. 3**). Considering that the surface area of stent-grafts is usually quite large (≥ 100 cm^2), reducing the costs associated with coating is an important advantage.

Another key result of this study is the important benefit of using CS as a sublayer for EGF immobilization. As assessed in the present study, the dense and homogenous CS layer created on aminated substrates displayed low fouling properties against EGF molecules (**Table 1**). Although CS has shown affinity for certain heparin-binding proteins [47], selective low adsorption of plasma proteins such as fibrinogen and albumin on CS-covered surfaces has also been reported by Keuren et al. [35]. This is of interest since low-fouling surfaces may optimize tethered growth factor bioactivity by preventing its denaturation and limiting plasma proteins adsorption [48]. The parallel study with carboxymethylated dextran (CMD), a well-known non-fouling surface, however showed a tremendous advantage of CS over dextran, on which

adhesion and survival were very low, even in the presence of immobilized EGF (**Fig. 4**). Poor cell adhesion and growth was already reported on bare PEG and dextran, presumably due to their cell resistance in addition to protein resistance [49, 50], and even in the presence of tethered EGF, a dense non-absorbent PEG layer prevented complete epithelialization [50]. In contrast, VSMC tend to adhere and spread on CS surfaces, with a network of actin stress fibers [12]. These differences are probably related to both the chemical composition and the chain structure of those polymers. Indeed, once grafted on the surface, free chain ends might repel more proteins in the case of branched polymers such as PEG and CMD compared to the loops of linear CS chains. Since integrin activation is known to cooperate with EGF receptor-signalling leading to enhanced and prolonged activation of downstream anti-apoptotic pathways such as ERK [51], it is likely that CS- mediated adhesion could synergize with EGF to enhance survival. Further work would be required to better explain cell adhesive properties of CS and identify integrin receptors responsible for VSMC adhesion on CS.

Other benefits of CS for SG surface modification are its non-thrombogenic and anticoagulant properties [35, 52] that could increase substrate access to the cells in vivo by preventing the formation of a dense blood clot barrier around the implant. Furthermore, introducing a CS-based coating seems to be consistent with a restoration of a healthy environment for aortic cells, since CS, among other GAGs, is severely reduced in aneurismal aorta [53]. Altogether, these features make CS as an ideal sublayer for growth factor immobilization.

While this study was carried out on aminated glass and microplates as model substrates for the ease of the demonstration, creation of similar bioactive coatings on realistic graft materials (PET, PTFE) is easy to achieve. Indeed, the amination of PET [31, 33, 34, 54] and PTFE [32, 34]

surfaces is easily achievable by aminolysis (for PET only) or by plasma processes ; we also recently reported the creation of uniform CS coatings on PET thanks to a primary-amine rich plasma polymerized coating [13]. Conclusions of this study are however limited by our in vitro model that may not mimic the in vivo pro-apoptotic environment. Future in vitro and in vivo testing will further assess the efficacy of our coating to improve healing around SG and limit aneurysm progression.

5. Conclusions

A method for growth factor oriented immobilization, involving two peptides binding to each other with high affinity, was successfully used to tether EGF on CS. The combination of a CS sublayer and oriented EGF greatly enhanced VSMC survival in serum-free conditions compared to randomly grafted EGF on CS, but also compared to EGF immobilized on non-fouling dextran surfaces. The superiority of the approach relies on 1) selective low fouling and cell adhesive properties of CS associated with 2) optimal orientation and higher density of EGF on the surface. The ultimate goal of this anti-apoptotic coating is to improve the healing around stent-grafts. Thanks to the versatility of the coil-based tethering strategy, co-capture of selected Ecoil-tagged growth factors on CS could be readily achieved to fine-tune implant bioactivity or target other applications, especially in tissue engineering scaffolds where nutrients and oxygen supplies are deficient before neovascularization occurs.

Acknowledgments

This work was supported by the Natural Sciences and Engineering Council of Canada (NSERC), the Canadian Institutes of Health Research (CIHR), the Canada Research Chairs on endovascular implants and biomaterials (S.L.) and protein-enhanced biomaterials (G.D.C.). We

also acknowledge a full scholarship (P.L.) grant from the Fonds de la Recherche Nature et Technologies Québec (FQRNT). The authors would also like to thank Charles Fortier for the production of Ecoil-EGF, Dr Nathalie Arbour for the use of the Synergy 4 Spectrophotometer, Dr Marie-Josée Hébert for the use of the digital camera and microscope (Leica DMLS microscope and Leica DFC420C camera).

Keywords

Biomaterials, chondroitin sulfate, EGF, oriented immobilization, VSMC survival.

References

1. Rahmany, M.B. and M. Van Dyke, *Acta biomaterialia*. **2013**, *9*(3), 5431-7.

2. Bogdanski, D., S.A. Esenwein, O. Prymak, M. Epple, G. Muhr, and M. Köller, *Biomaterials*. **2004**, *25*(19), 4627-4632.

3. Parodi, J.C., J.C. Palmaz, and H.D. Barone, *Annals of Vascular Surgery*. **1991**, *5*(6), 491-499.

4. Major, A., R. Guidoin, G. Soulez, L.A. Gaboury, G. Cloutier, M. Sapoval, Y. Douville, G. Dionne, R.H. Geelkerken, P. Petrasek, and S. Lerouge, *Journal of Endovascular Therapy*. **2006**, *13*(4), 457-467.

5. Szilagyi, D.E., *Journal of Vascular Surgery*. **2001**, *33*(6), 1283-1285.

6. McArthur, C., V. Teodorescu, L. Eisen, N. Morrissey, P. Faries, L. Hollier, and M.L. Marin, *Journal of Vascular Surgery*. **2001**, *33*(4), 733-738.

7. Bennett, M.R. and J.J. Boyle, *Atherosclerosis*. **1998**, *138*(1), 3-9.

8. Rowe, V.L., S.L. Stevens, T.T. Reddick, M.B. Freeman, R. Donnell, R.C. Carroll, and M.H. Goldman, *Journal of Vascular Surgery*. **2000**, *31*(3), 567-576.

9. Theocharis, A.D., I. Tsolakis, T. Tsegenidis, and N.K. Karamanos, *Atherosclerosis*. **1999**, *145*(2), 359-368.

10. Choke, E., G. Cockerill, W.R.W. Wilson, S. Sayed, J. Dawson, I. Loftus, and M.M. Thompson, *European Journal of Vascular and Endovascular Surgery*. **2005**, *30*(3), 227-244.

11. Charbonneau, C., J.E. Gautrot, M.J. Hebert, X.X. Zhu, and S. Lerouge, *Macromolecular Bioscience*. **2007**, *7*(5), 746-752.

12. Charbonneau, C., B. Liberelle, M.-J. Hébert, G. De Crescenzo, and S. Lerouge, *Biomaterials*. **2011**, *32*(6), 1591-1600.

13. Charbonneau, C., J.C. Ruiz, P. Lequoy, M.J. Hebert, G. De Crescenzo, M.R. Wertheimer, and S. Lerouge, *Macromolecular Bioscience*. **2012**, *12*(6), 812-821.

14. Raymond, M.A., A. Desormeaux, P. Laplante, N. Vigneault, J.G. Filep, K. Landry, A.V. Pshezhetsky, and M.J. Hebert, *Faseb Journal*. **2004**, *18*(2), U166-U184.

15. Laplante, P., M.A. Raymond, G. Gagnon, N. Vigneault, A.M.J. Sasseville, Y. Langelier, M. Bernard, Y. Raymond, and M.J. Hebert, *Journal of Immunology*. **2005**, *174*(9), 5740-5749.

16. Hinek, A., J. Boyle, and M. Rabinovitch, *Experimental Cell Research*. **1992**, *203*(2), 344-353.

17. Zou, X.H., Y.Z. Jiang, G.R. Zhang, H.M. Jin, N.T.M. Hieu, and H.W. Ouyang, *Acta Biomaterialia*. **2009**, *5*(5), 1588-1595.

18. Barrientos, S., O. Stojadinovic, M.S. Golinko, H. Brem, and M. Tomic-Canic, *Wound Repair and Regeneration*. **2008**, *16*(5), 585-601.

19. Buckley, A., J.M. Davidson, C.D. Kamerath, T.B. Wolt, and S.C. Woodward, *Proceedings of the National Academy of Sciences*. **1985**, *82*(21), 7340-7344.

20. Kaiura, T.L., H. Itoh, S.M. Kubaska Iii, T.A. McCaffrey, B. Liu, and K. Craig Kent, *Journal of Vascular Surgery*. **2000**, *31*(3), 577-584.

21. Major, T.C. and J.A. Keiser, *Journal of Pharmacology and Experimental Therapeutics*. **1997**, *283*(1), 402-410.

22. Upchurch, G.R., *Circulation*. **2005**, *112*(7), 939-940.

23. Henson, E.S. and S.B. Gibson, *Cellular Signalling*. **2006**, *18*(12), 2089-2097.

24. Ying, W.Z., H.G. Zhang, and P.W. Sanders, *Journal of the American Society of Nephrology*. **2007**, *18*(1), 131-142.

25. Soulez, M., I. Sirois, N. Brassard, M.A. Raymond, F. Nicodeme, N. Noiseux, Y. Durocher, A.V. Pshezhetsky, and M.J. Hebert, *Stem Cells*. **2010**, *28*(4), 810-820.

26. Kuhl, P.R. and L.G. Griffith-Cima, *Nature Medicine*. **1996**, *2*(9), 1022-1027.

27. Liberelle, B., C. Boucher, J.K. Chen, M. Jolicoeur, Y. Durocher, and G. De Crescenzo, *Bioconjugate Chemistry*. **2010**, *21*(12), 2257-2266.

28. Boucher, C., G. St-Laurent, M. Loignon, M. Jolicoeur, G. De Crescenzo, and Y. Durocher, *Tissue Engineering Part A*. **2008**, *14*(12), 2069-2077.

29. Boucher, C., J.-C. Ruiz, M. Thibault, M.D. Buschmann, M.R. Wertheimer, M. Jolicoeur, Y. Durocher, and G. De Crescenzo, *Biomaterials*. **2010**, *31*(27), 7021-7031.

30. Liberelle, B., A. Merzouki, and G.D. Crescenzo, *Journal of Immunological Methods*. **2013**, *389*(1–2), 38-44.

31. Bech, L., T. Meylheuc, B. Lepoittevin, and P. Roger, *Journal of Polymer Science Part A: Polymer Chemistry*. **2007**, *45*(11), 2172-2183.

32. Kang, E.T., K.L. Tan, K. Kato, Y. Uyama, and Y. Ikada, *Macromolecules*. **1996**, *29*(21), 6872-6879.

33. Noel, S., B. Liberelle, L. Robitaille, and G. De Crescenzo, *Bioconjugate Chemistry*. **2011**, *22*(8), 1690-1699.

34. Lerouge, S., A. Major, P.-L. Girault-Lauriault, M.-A. Raymond, P. Laplante, G. Soulez, F. Mwale, M.R. Wertheimer, and M.-J. Hébert, *Biomaterials*. **2007**, *28*(6), 1209-1217.

35. Keuren, J.F.W., S.J.H. Wielders, G.M. Willems, M. Morra, L. Cahalan, P. Cahalan, and T. Lindhout, *Biomaterials*. **2003**, *24*(11), 1917-1924.

36. Resch, T., K. Ivancev, J. Brunkwall, U. Nyman, M. Malina, and B. Lindblad, *Journal of Vascular and Interventional Radiology*. **1999**, *10*(3), 257-264.

37. Malina, M., B. Lindblad, K. Ivancev, M. Lindh, J. Malina, and J. Brunkwall, *Journal of Endovascular Surgery*. **1998**, *5*(4), 310-317.

38. van der Bas, J.M.A., P.H.A. Quax, A.C. van den Berg, M.J.T. Visser, E. van der Linden, and J.H. van Bockel, *Journal of Vascular Surgery*. **2004**, *39*(4), 850-858.

39. Kajimoto, M., T. Shimono, K. Hirano, Y. Miyake, N. Kato, K. Imanaka-Yoshida, H. Shimpo, and K. Miyamoto, *Journal of Vascular Surgery*. **2008**, *48*(5), 1306-1314.

40. van der Bas, J.M.A., P.H.A. Quax, A.C. van den Berg, V.W.M. van Hinsbergh, and J.H. van Bockel, *Journal of Vascular Surgery*. **2002**, *36*(6), 1237-1247.

41. Kader, K.N. and C.M. Yoder, *Materials Science and Engineering: C*. **2008**, *28*(3), 387-391.

42. Wells, A., K. Gupta, P. Chang, S. Swindle, A. Glading, and H. Shiraha, *Microscopy Research and Technique*. **1998**, *43*(5), 395-411.

43. Xie, H., M.A. Pallero, K. Gupta, P. Chang, M.F. Ware, W. Witke, D.J. Kwiatkowski, D.A. Lauffenburger, J.E. Murphy-Ullrich, and A. Wells, *Journal of Cell Science*. **1998**, *111*, 615-624.

44. Jorissen, R.N., F. Walker, N. Pouliot, T.P.J. Garrett, C.W. Ward, and A.W. Burgess, *Experimental Cell Research*. **2003**, *284*(1), 31-53.

45. Bitterman, P.B. and C.A. Henke, *CHEST Journal*. **1991**, *99*(3_Supplement), 81S-84S.

46. Bennett, M.R. and M. O'Sullivan, *Pharmacology & Therapeutics*. **2001**, *91*(2), 149-166.

47. Sugahara, K., T. Mikami, T. Uyama, S. Mizuguchi, K. Nomura, and H. Kitagawa, *Current Opinion in Structural Biology*. **2003**, *13*(5), 612-620.

48. Goddard, J.M. and J.H. Hotchkiss, *Progress in Polymer Science*. **2007**, *32*(7), 698-725.

49. Massia, S.P., J. Stark, and D.S. Letbetter, *Biomaterials*. **2000**, *21*(22), 2253-2261.

50. Klenkler, B.J., H. Chen, Y. Chen, M.A. Brook, and H. Sheardown, *Journal of Biomaterials Science-Polymer Edition*. **2008**, *19*(11), 1411-1424.

51. Miyamoto, S., H. Teramoto, J.S. Gutkind, and K.M. Yamada, *The Journal of Cell Biology*. **1996**, *135*(6), 1633-1642.

52. McGee, M. and W.D. Wagner, *Arteriosclerosis Thrombosis and Vascular Biology*. **2003**, *23*(10), 1921-1927.

53. Theocharis, A.D., D.A. Theocharis, G. De Luca, A. Hjerpe, and N.K. Karamanos, *Biochimie*. **2002**, *84*(7), 667-674.

54. Girardeaux, C., N. Zammatteo, M. Art, B. Gillon, J.J. Pireaux, and R. Caudano, *Plasmas and Polymers*. **1996**, *1*(4), 327-346.

Figures

Figure 1. Schematic illustration of the grafting steps for the oriented EGF immobilization on CS and CMD. The grafting of CS or CMD layers on aminated surfaces was followed by the chemical grafting of cysteine-tagged Kcoil peptides using EMCH as heterobifunctional linker. Remaining EMCH thiol-reactive groups were deactivated using cysteine molecules. Ecoil-tagged EGF proteins were captured on the surface via the reversible E/K coiled-coil interaction.

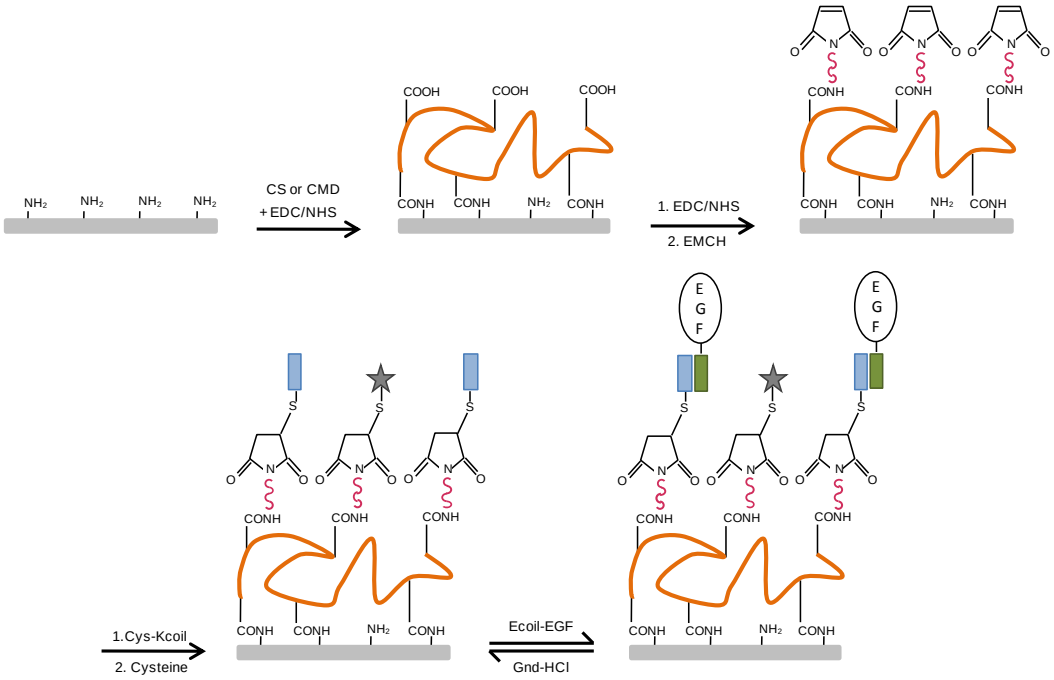

CMD	R= -CH2-COOH (55%) or -OH (45%)		Cys-Kcoil	$CGG-[KVSALKE]_5$	SH
CS			Ecoil-EGF	$[EVSALEK]_5$ - EGF	E G F
EMCH		NH_2	Cysteine		SH

Figure 2. Sequential grafting of Ecoil-EGF on CS-coated surfaces via coiled-coil interactions followed by dry thickness measured by ellipsometry. (a) APTES; (b) APTES+CS; (c) APTES+CS+EMCH+Kcoil+cysteine; (d) Ecoil-EGF capture on (c); (e) Ecoil-EGF removal after capture (as in d) with guanidium hydrochloride (5 M). As a negative control (g), Ecoil-EGF was incubated on (f) cysteine-blocked EMCH layers (no Kcoil). The reference was set as (0 nm, 0°) for a cleaned silicon wafer surface. (n = 3)

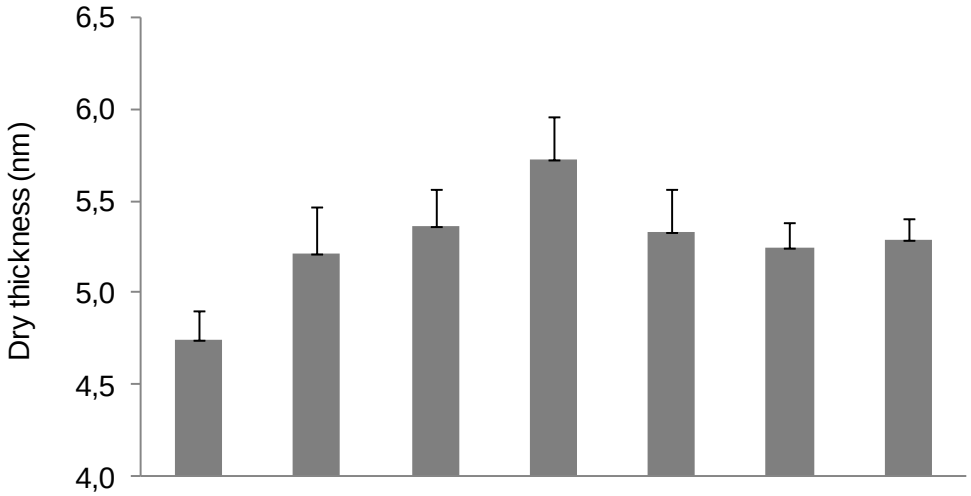

	a	b	c	d	e	f	g
APTES	+	+	+	+	+	+	+
CS		+	+	+	+	+	+
EMCH			+	+	+	+	+
Kcoil			+	+	+		
Cysteine				+	+	+	+
Ecoil-EGF				+	+		+
Gnd/HCl					+		

Figure 3. Variation of EGF surface density on CS and CMD with Ecoil-tagged or untagged EGF concentration during incubation. Apparent surface densities for oriented and randomly grafted EGF were evaluated by direct ELISA ($n \geq 8$).

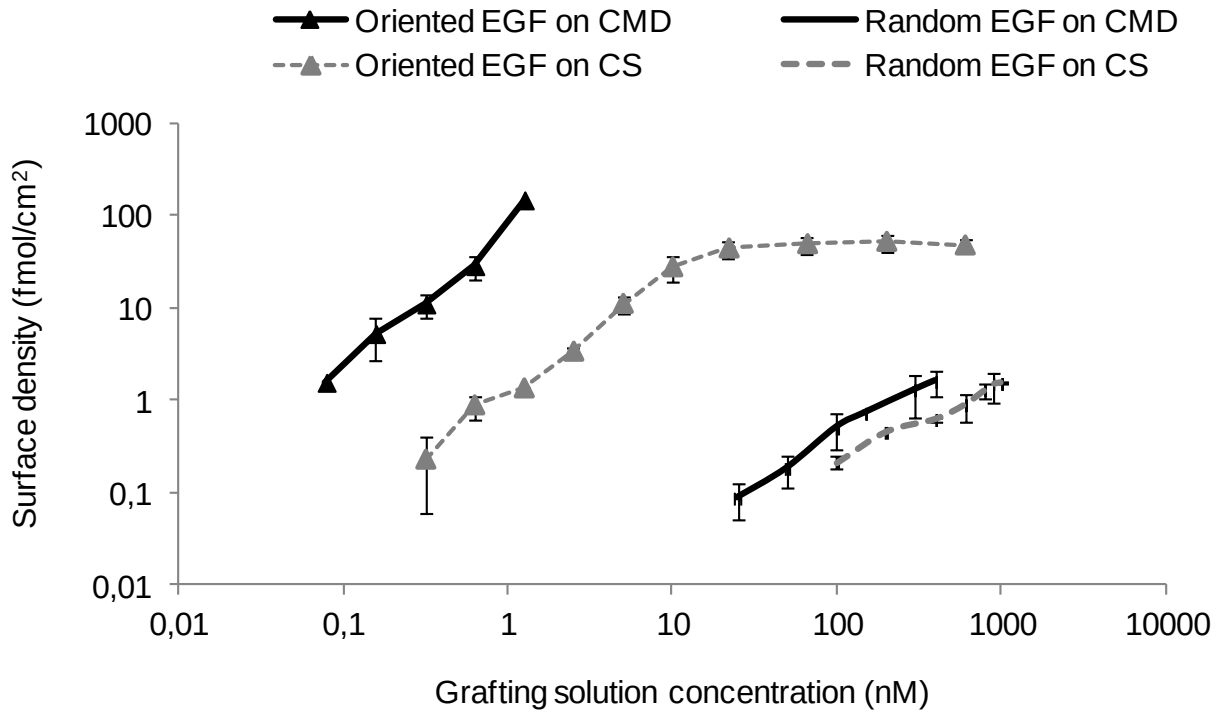

Figure 4. VSMC adhesion after 24h in complete growth medium. VSMC adhesion was expressed (in %) as alamarBlue signal at D0 on each surface normalized to the signal at day 0 on PS (100%). Soluble EGF (Sol. EGF) was added at 10 ng/mL in culture medium. EGF surface densities on CS and CMD were identical, respectively 1.5 fmol/cm^2 for random immobilization (Rand. EGF) and 45 fmol/cm^2 for oriented immobilization (Ori. EGF). Statistical difference noticed * $p < 0.005$.

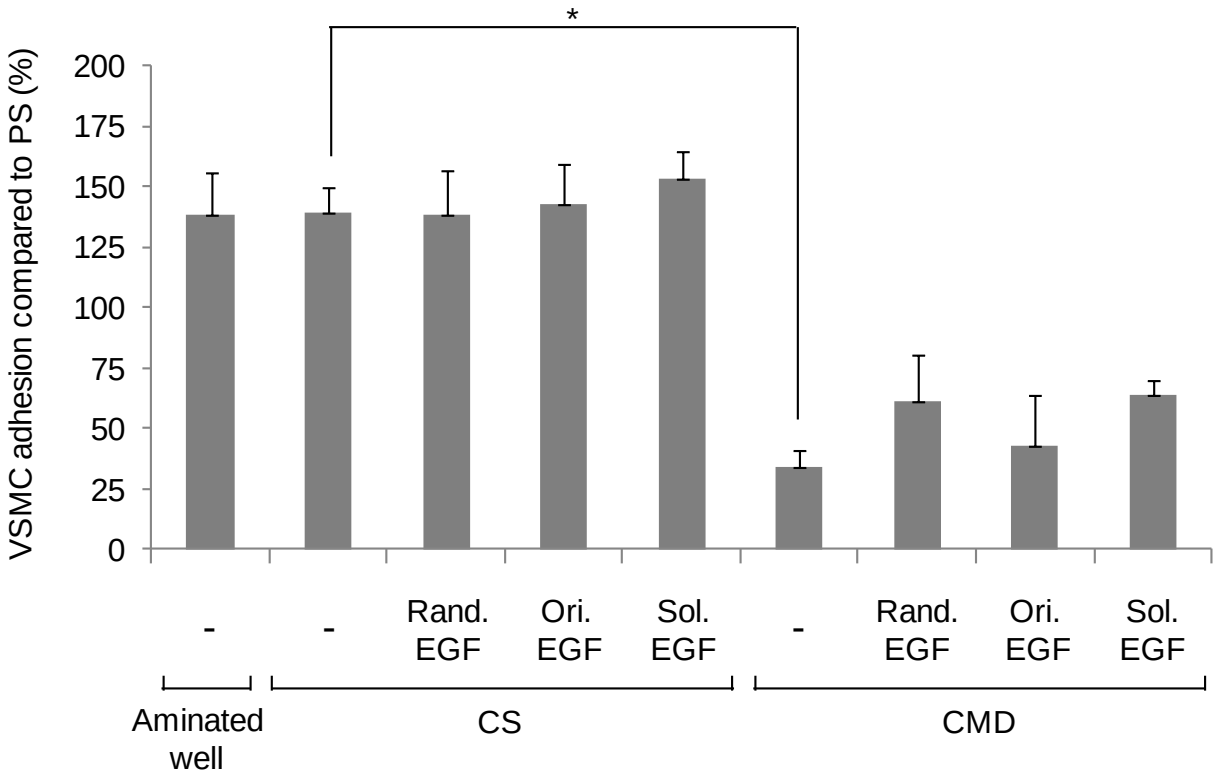

Figure 5. VSMC survival in serum-free conditions. After 24h in complete growth medium for adhesion (D0), cells were exposed to serum-free medium for 3, 5 or 7 days (D3, D5 and D7). VSMC survival (in %) was expressed as a ratio of alamarBlue signal at day 3, 5 and 7 to the signal at day 0 on the same surface. Soluble EGF (Sol. EGF) was added at 10 ng/mL in culture medium. EGF surface densities on CS and CMD were identical, i.e. 1.5 and 45 fmol/cm^2 for random (Rand. EGF) and oriented immobilization (Ori. EGF), respectively. Statistical differences between random and oriented EGF on CS were *: $p = 0.01$ at D3, **: $p < 0.0001$ at day 5 and 7 ($n \geq 8$).

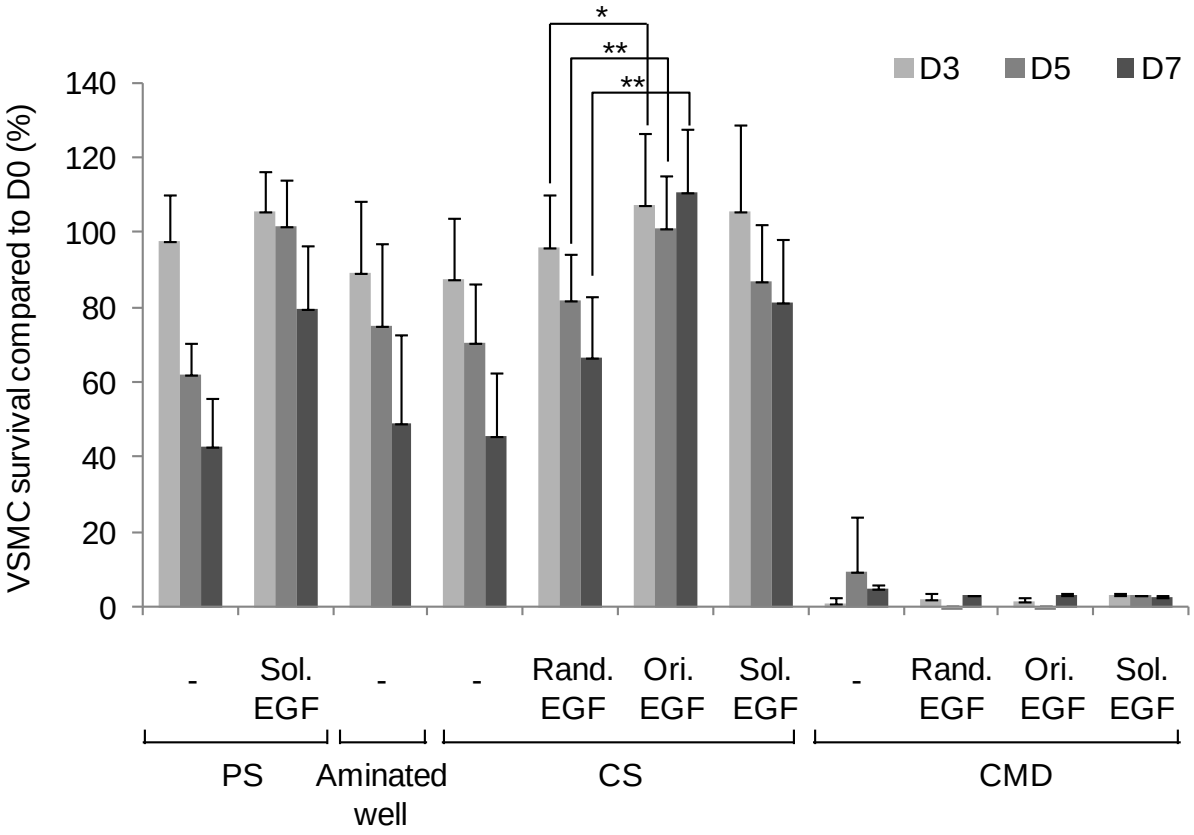

Figure 6. VSMC density and homogeneity observed by crystal violet staining. After 24h adhesion in complete growth medium, cells were left for 7 days in serum-free conditions. Soluble EGF concentration (10 ng/mL) and surface EGF densities (1.5 fmol/cm^2 for random grafting and 45 fmol/cm^2 for oriented tethering) were identical for all substrates. Scale bars correspond to 200 µm.

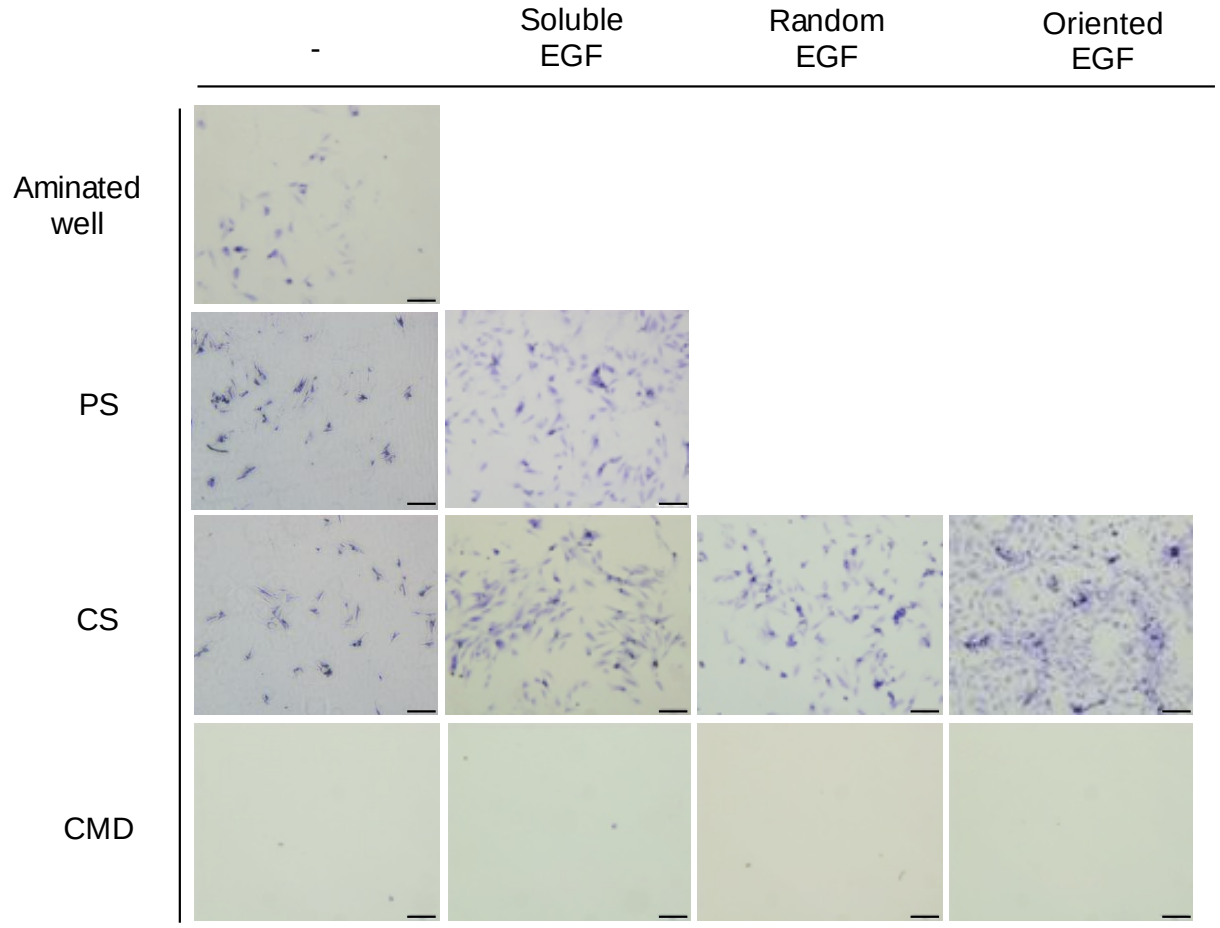

Figure 7. Percentages of apoptotic and necrotic VSMC in serum-free conditions. After 8h in complete growth medium for adhesion, the cells were exposed to either complete (control) or serum-free (pro-apoptotic) medium for 14h. Apoptotic and necrotic cells were counted after Hoescht 33342/propidium iodide staining, and percentages were obtained by the ratio of apoptotic (or necrotic) cells over total number of cells. Statistical differences were *: $p < 0.005$ between CS and PS**: $p = 0.2$ between CS and random EGF (Rand. EGF) and ***: $p = 0.01$ between CS and oriented EGF (Ori. EGF) ($n = 8$).

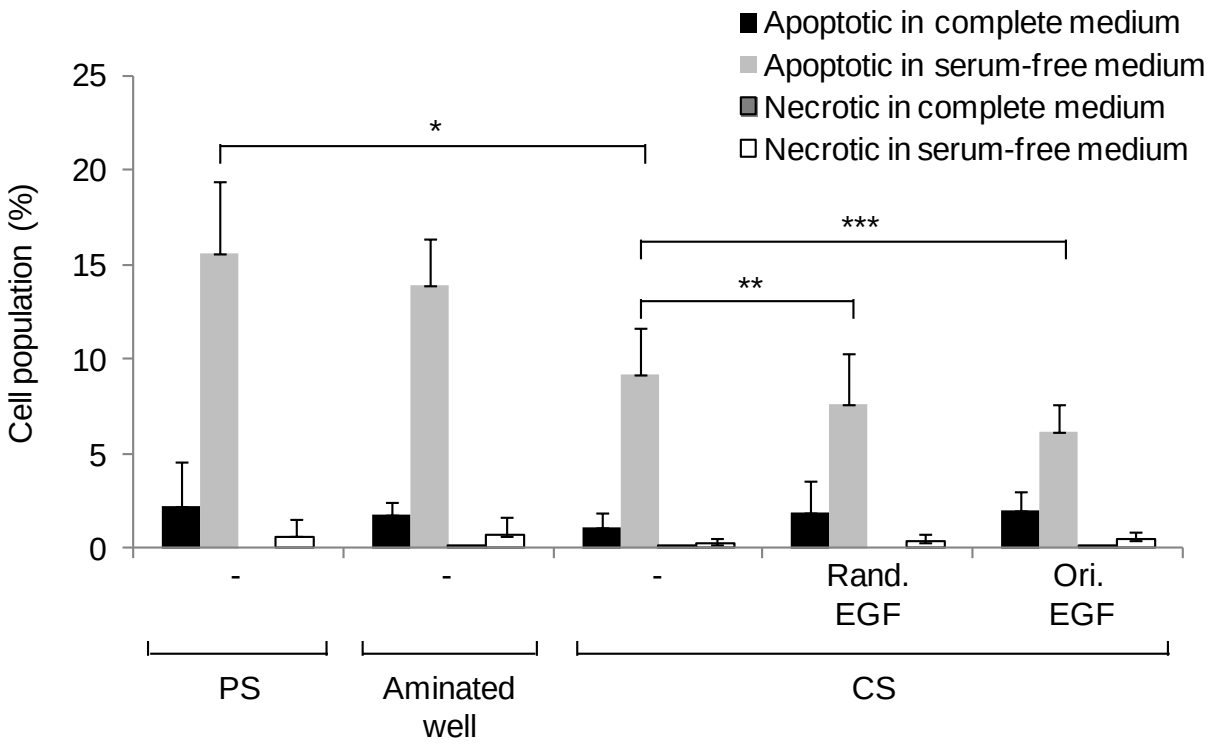

Table 1. Non-specific adsorption of EGF measured by ELISA. EGF was incubated at 100 nM (in PBS) for 1h on bare aminated microplate wells, CS and CMD (Mean ± standard deviation; $n \geq 4$). Statistical differences were *: $p < 0.001$ between CS and aminated wells, and CMD and aminated wells. No statistical differences were found between CS and CMD ($p = 0.62$).

	CS	CMD	Aminated wells
Surface density of adsorbed EGF (fmol/cm^2)	0.077 ± 0.003*	0.070 ± 0.024*	0.934 ± 0.154

Table of contents

An anti-apoptotic coating created by oriented immobilization of EGF via coiled-coil peptides was shown to display higher protein surface densities and bioactivity compared to random grafting. In addition, the huge benefit of chondroitin sulfate as a sublayer for growth factor immobilization was highlighted by comparison with another low-fouling surface.